Electronic Supplementary Material (ESI) for Journal of Materials Chemistry C.

Supplementary Material

Adjusting the energy gap and interface effect of titania nanosheets synergistically enhances the energy storage performance of PVDF based composites

Congcong Zhu,[ab] Xiaoxu Liu,*[a] Yu Feng,[c] Jialong Li,[a] Yanpeng Li,[b] He Zhao,[c] Dong Yue [b] and Jinghua Yin *[bc]

[a] School of Material Science and Engineering, Shaanxi University of Science and Technology, Xi'an, 710021, China.

[b] School of Material Science and Chemical Engineering, Harbin University of Science and Technology, Harbin 150080, P. R. China.

[c] Key Laboratory of Engineering Dielectrics and Its Application, Ministry of Education, Harbin University of Science and Technology, Harbin 150080, P. R. China.

Correspondence to：*E-mail: xiaoxuliu@sust.edu.cn, **E-mail: yinjinghua1@126.com

Experimental

Material

Poly(vinylidene fluoride) (PVDF) powder with the number-average molecular weight of 534 000 was provided by Sigma-Aldrich Co., Ltd. (Shanghai, China). Potassium carbonate (K_2CO_3), lithium carbonate (Li_2CO_3), Rutile titania nanoparticles (TiO_2, diameter of 60 nm), tetramethylammonium hydroxide (TMAOH) and tetrabutylammonium hydroxide (TBAOH) were purchased from Aladdin Industrial Corporation. The N, N-dimethylformamide (DMF) and anhydrous ethanol were provided by Tianjin Fuyu Fine Co., Ltd. (Tianjing, China).

Preparation of LTNSs and STNSs

LTNSs and STNSs were synthesized via the top-down exfoliation method.[1] The process scheme for the nanosheets is described and shown in Figure S2. Especially, the large titania nanosheets (LTNSs) with a lateral size of 11-59 μm were fabricated in our previous work.[2] In order to prepare smaller titania nanosheets compared with LTNSs, the calcination time of 20 hours was changed to 2 hours. And the TBAOH were used as the electrolyte instead of TMAOH. The lateral size of small titania nanosheets (STNSs) is about 0.9-2.8 μm.

Preparation of the composites

Pure PVDF and PVDF/TNSs composites (0.5, 1.5 and 2 wt%) were prepared via simple physical blending and hot-press method.[3] The appropriate amount of TNSs were dissolved in 7 ml DMF solvent by sonication and then mixed with PVDF powder of 1 g for further stirring for 24 h. The suspension was poured into a clean glass, and dried at 80 °C for 10 h. Finally, the samples were hot-pressed at 180 °C for 30 min under 15 MPa pressure. The thickness of the final composite films was approximately 20±5 μm.

Characterization

The microstructure and morphology of TNSs and PVDF/TNSs composites were investigated by scanning electron microscopy (SEM, Hitachi SU8020) and atomic force microscope (AFM). The AFM was measured into samples using a Nanoscope V Multimode 8 scanning probe microscope from Bruker Corporation. The lateral resolution of the AFM is about 1 nm, and the vertical resolution is about 0.1 nm. The wide-angle X-ray diffraction (XRD) tests using Bruker D8 Advance with a scan range (2θ) of 5°-80°. Fourier transform infrared spectroscopy (FTIR) experiments were carried out using a JASCO 6100 equipment. The small angle x-ray scattering (SAXS) experiments were measured

to research the microstructure of the composites at the beam line 1W2A in Beijing Synchrotron Radiation Facility. The thermal transition data was recorded by a DSC (differential scanning calorimeter, Mettler Toledo model DSC-1) with heating rate of 10 °C/min under N_2 flow. Dielectric properties were tested at the frequency range of 1 Hz to 1 MHz via the broadband impedance analyzer (GmbH Novocontrol Alpha-A). Besides, the effects of temperature on dielectric performance of the composites were performed from 80 to 110 °C. The breakdown strength tests of composites were carried out via YDZ-560. The polarization-electric field (*P*-*E*) loops of the composites were measured using the Radiant Premier II Ferroelectric Test System at frequency of 100 Hz. Leakage current density was also collected by this equipment at frequency of 10 Hz.

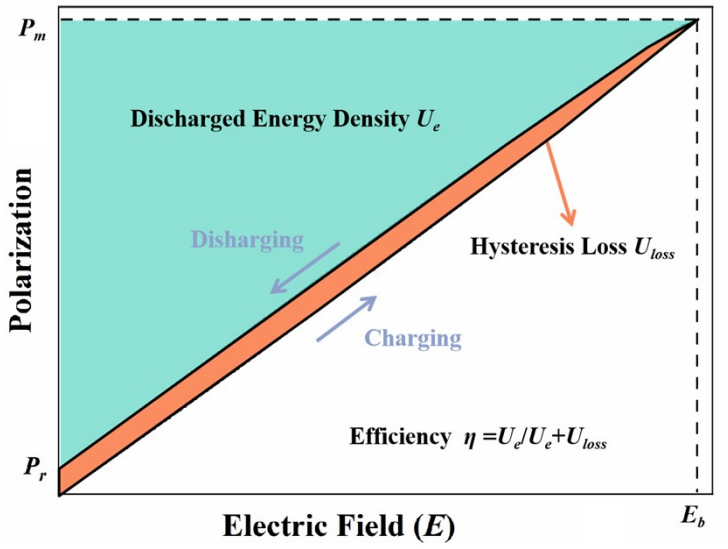

Figure S1. Schematic of polymer dielectric energy storage.

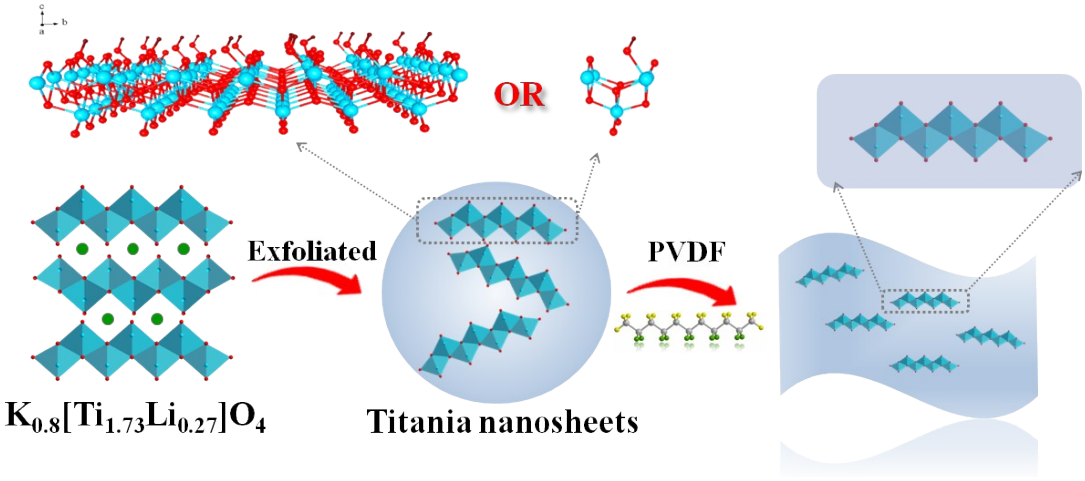

Figure S2. (a) Fabrication routes for LTNSs, STNSs and PVDF/TNSs composite films.

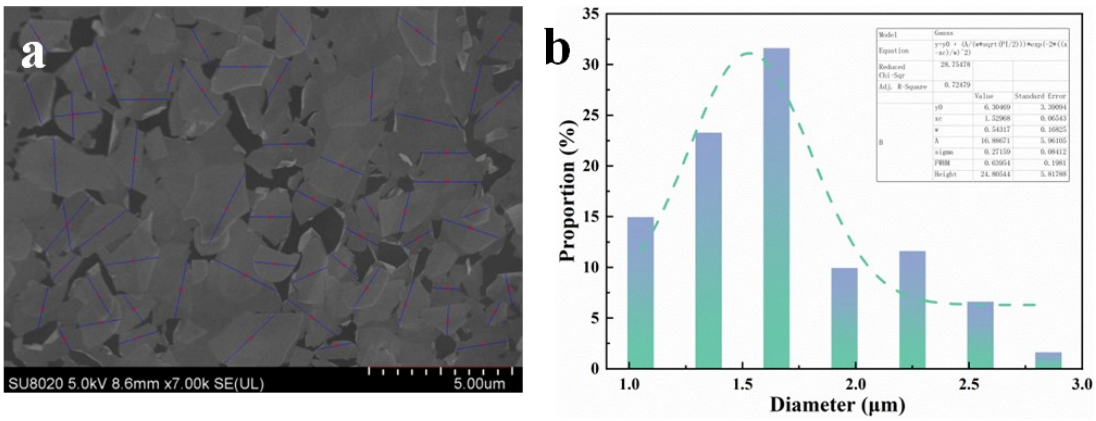

Figure S3. (a) Measured STNSs and (b)statistical curve of aspect ratio in SEM image.

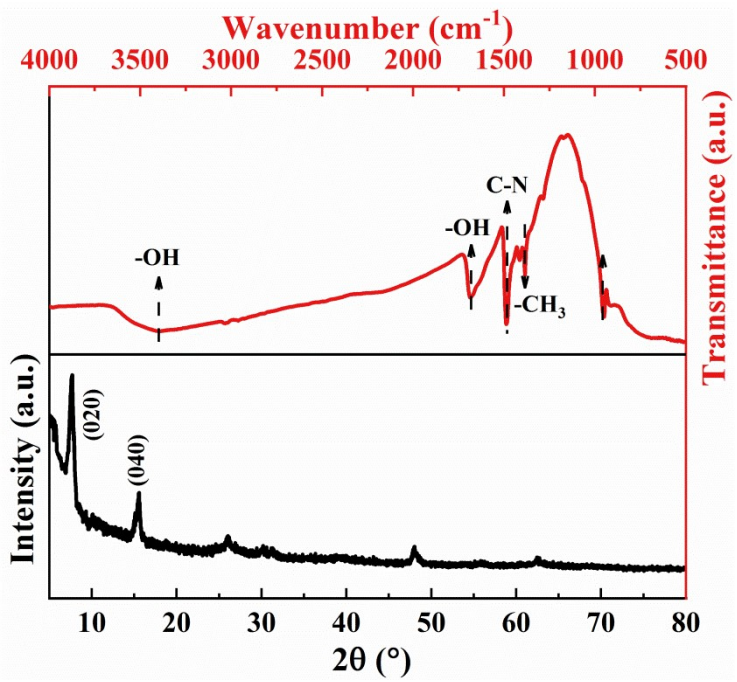

Figure S4. FTIR and XRD of LTNSs.

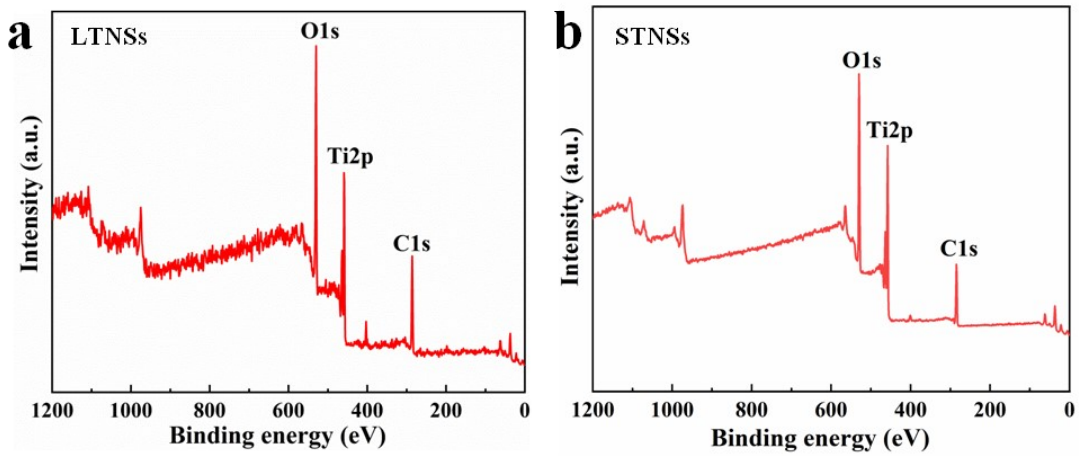

Figure S5. The XPS spectrum of LTNSs and STNSs.

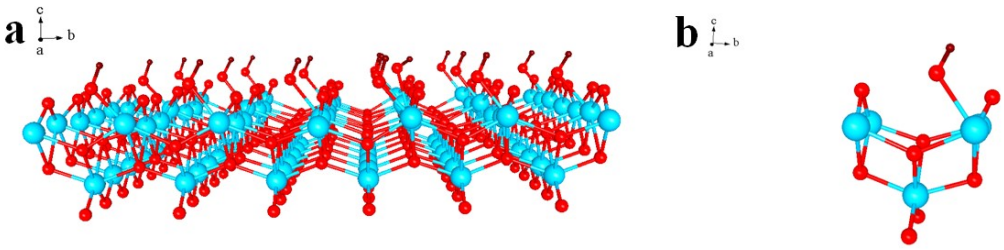

Figure S6. (a), (b) Crystal structures of TNSs with different sizes.

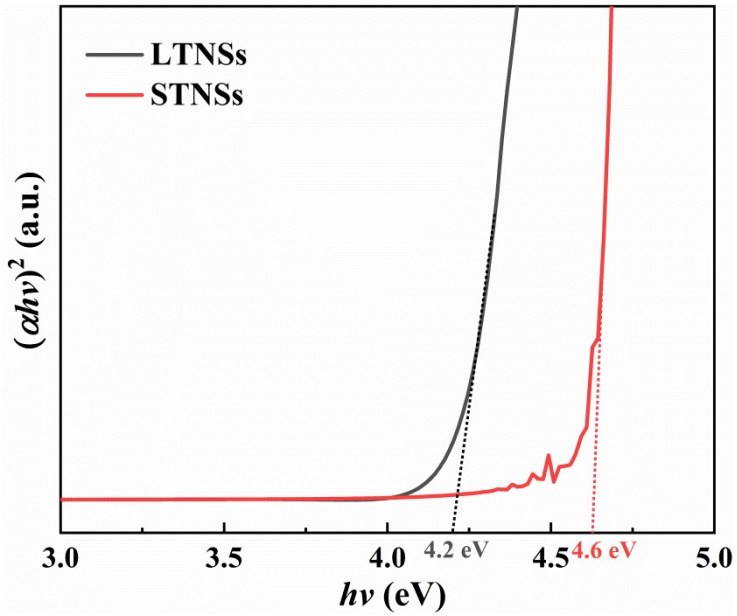

Figure S7. (Ahv)^2-hv plots of TNSs .

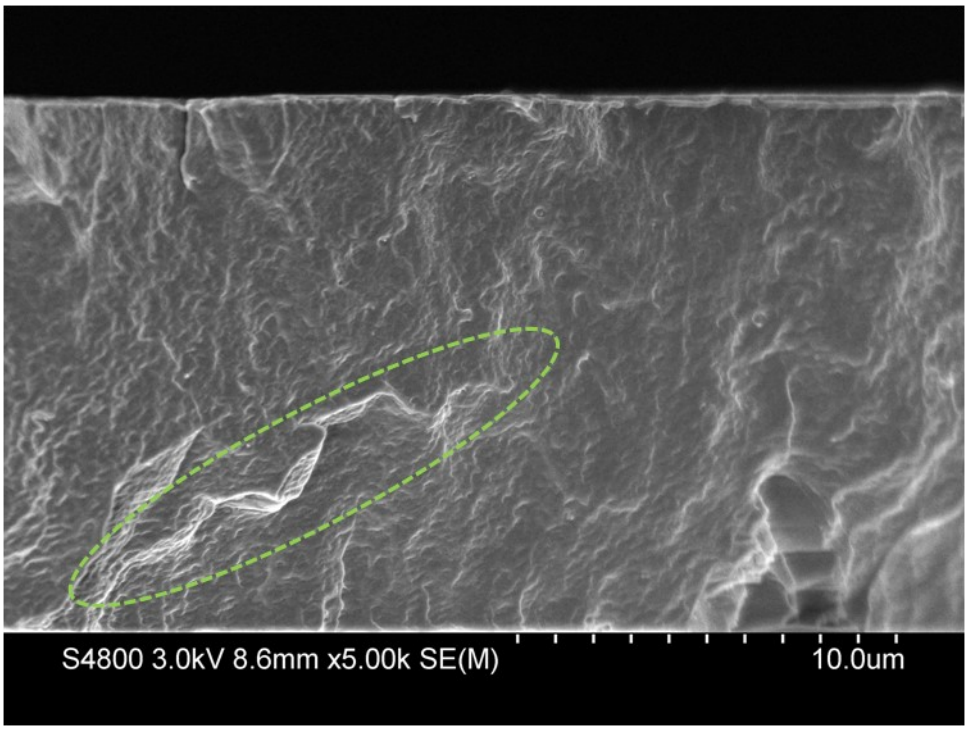

Figure S8. Cross-sectional SEM image of PVDF/LTNSs composite with 0.5 wt%.

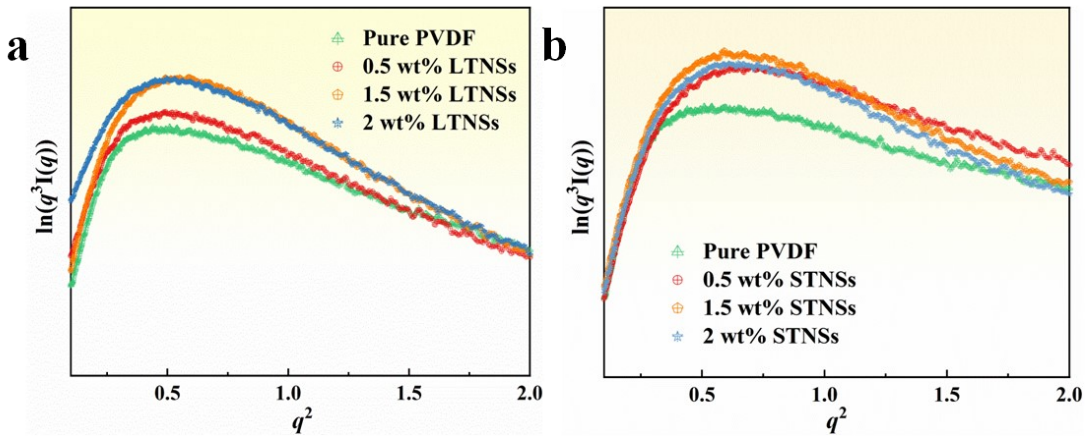

Figure S9. Porod curves of PVDF/TNSs composites.

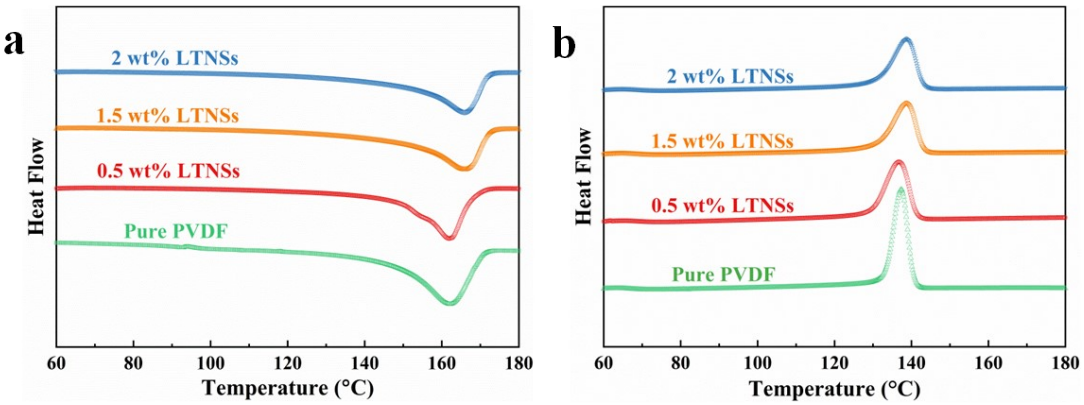

Figure S10. The DSC (a) endothermic curves and (b) exothermic curves of pure PVDF and the PVDF/LTNSs composites.

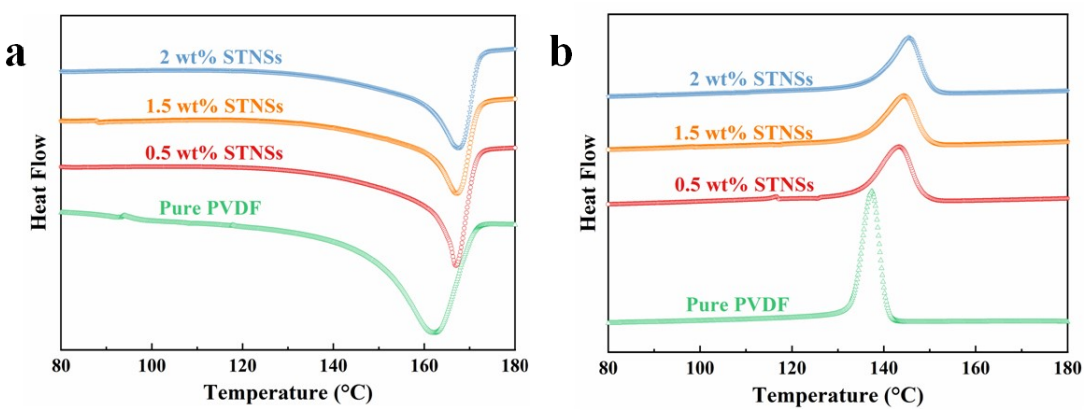

Figure S11. The DSC (a) endothermic curves and (b) exothermic curves of pure PVDF and the PVDF/STNSs composites.

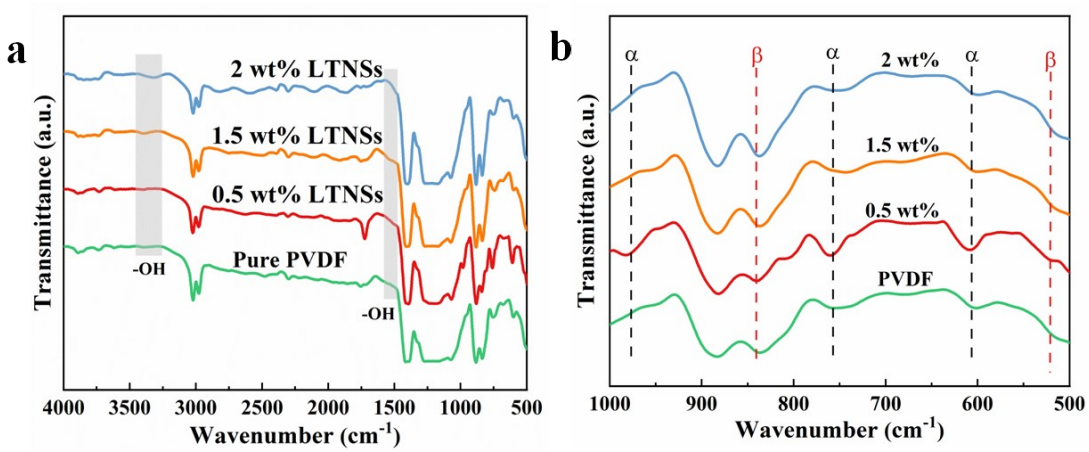

Figure S12. (a) FTIR spectra, (b) FTIR spectra at wavenumber=500-1000 cm^{-1} of PVDF/LTNSs composites.

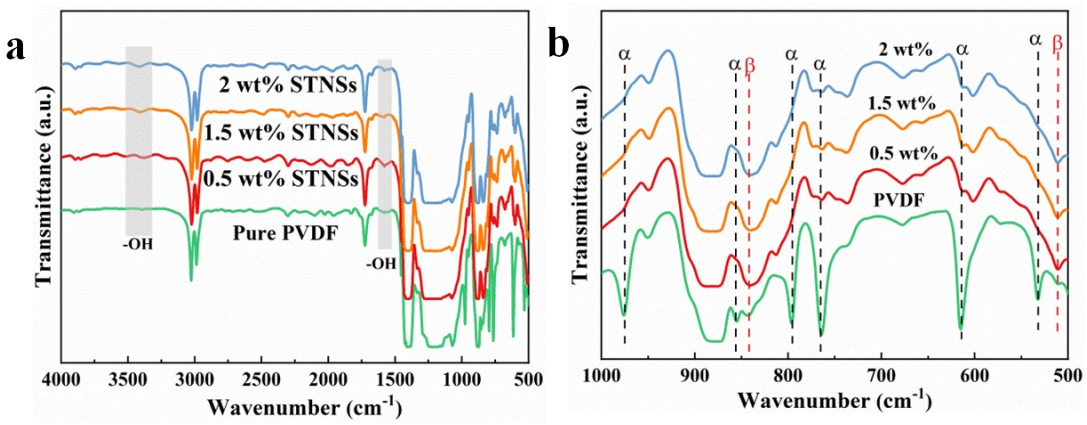

Figure S13. The FTIR spectra, (a) FTIR spectra at wavenumber=500-1000 cm^{-1} of pure PVDF and the PVDF/STNSs composites.

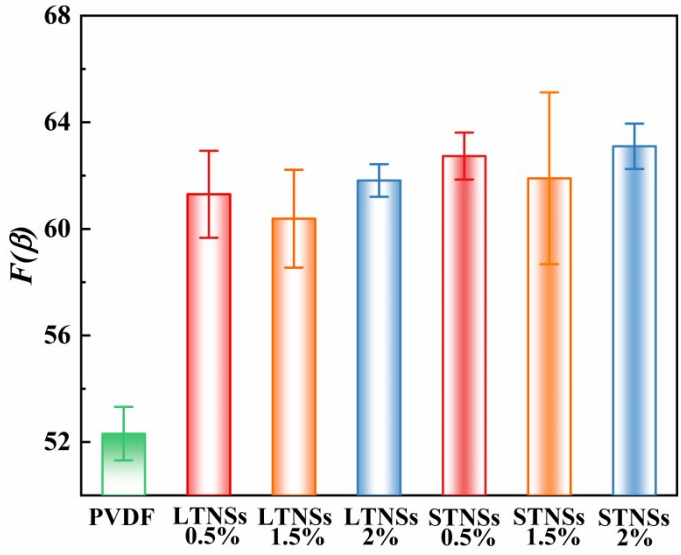

Figure S14. *F(β)* of PVDF/TNSs composites.

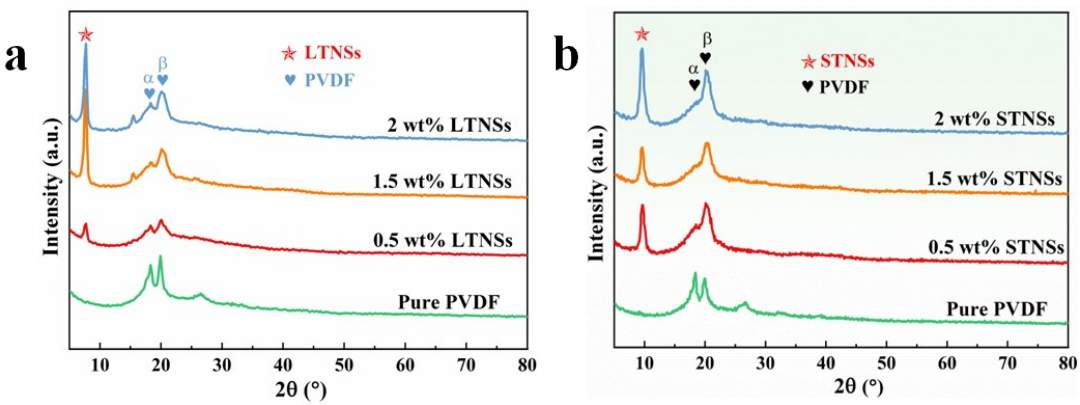

Figure S15. XRD patterns of PVDF/TNSs composites.

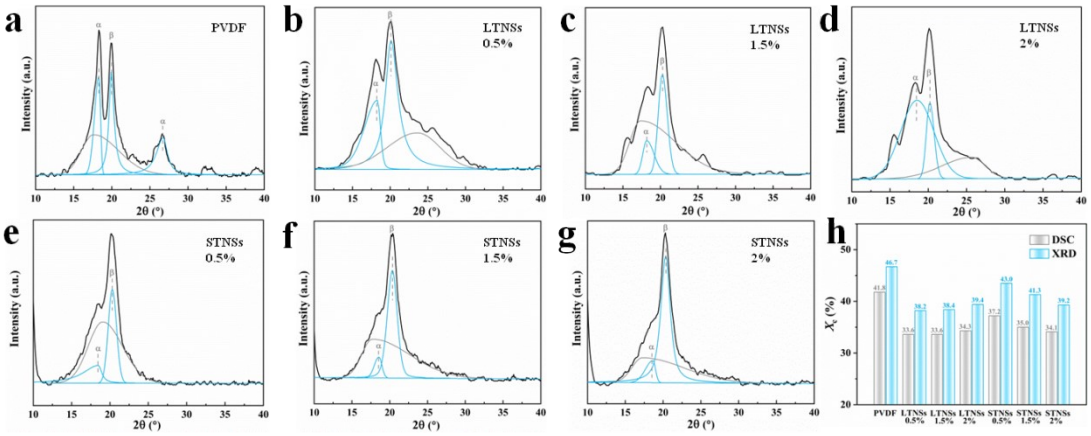

Figure S16. (a)-(g) The deconvolution of the XRD data of PVDF/TNSs composites. (h) The crystallinity X_c of pure PVDF and PVDF/TNSs composites.

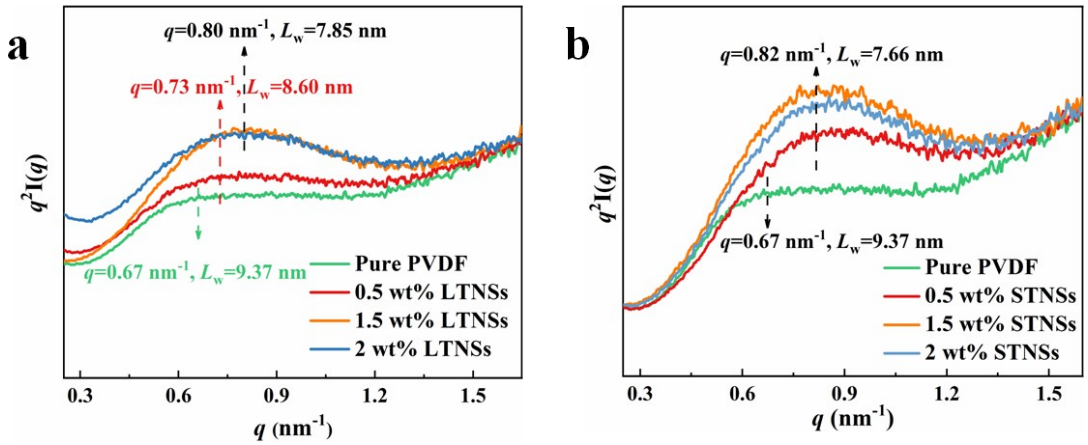

Figure S17. Lorentz-corrected SAXS profiles of PVDF/TNSs composites.

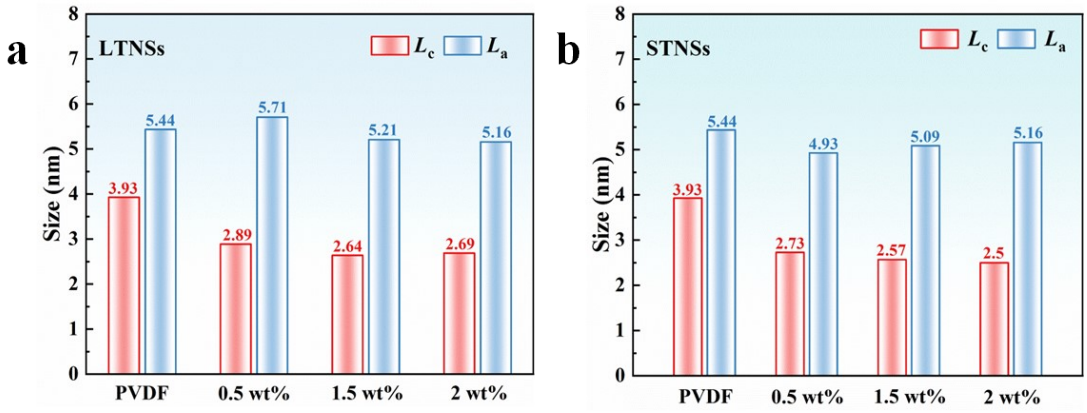

Figure S18. L_c and L_a of PVDF/TNSs composites.

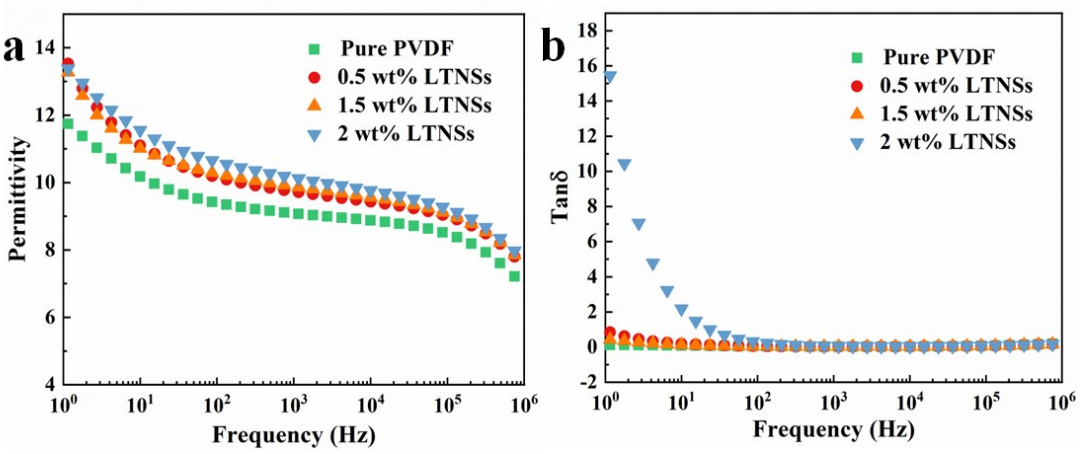

Figure S19. Dielectric permittivity and loss tangent curves of pure PVDF and the PVDF/LTNSs composites.

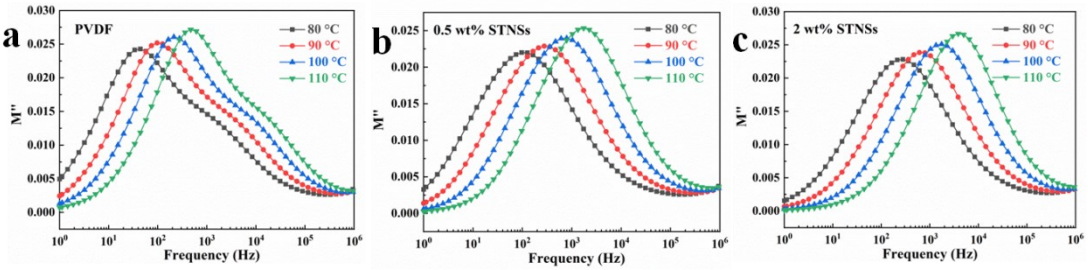

Figure S20. Frequency dependence of the imaginary electric modulus (*M''*) of (a) PVDF, (b) 0.5 wt% and (c) 2 wt% PVDF/STNSs composites.

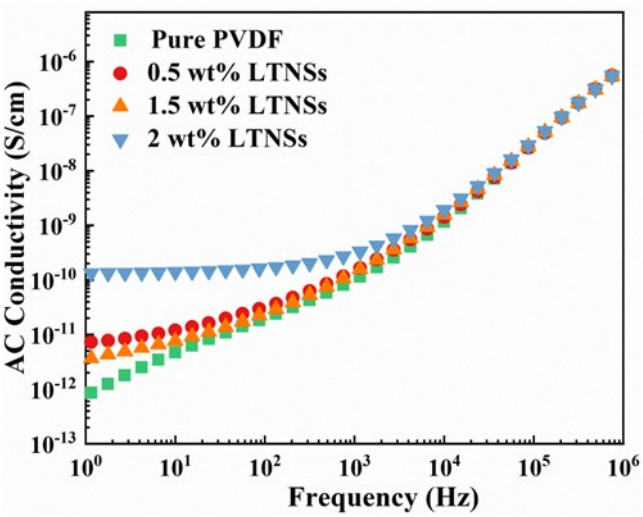

Figure S21. AC conductivity of PVDF/LTNSs composites.

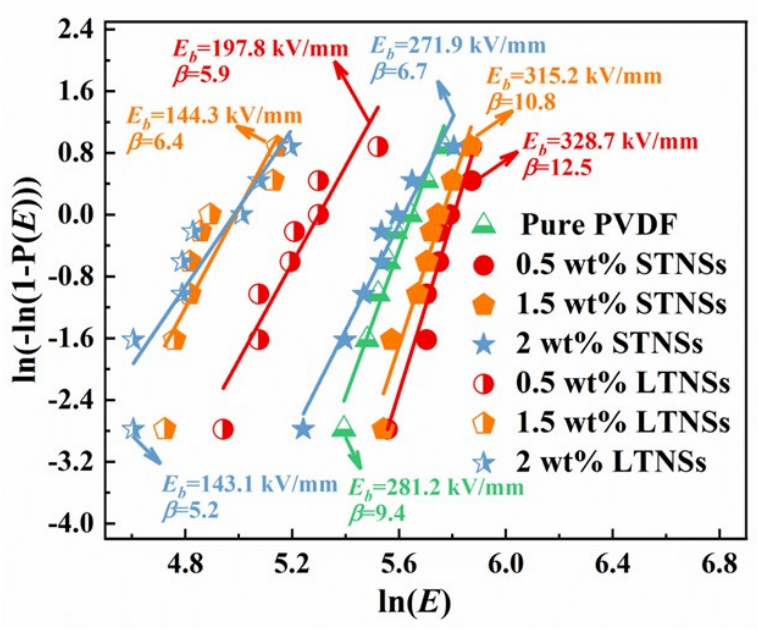

Figure S22. The breakdown strength of PVDF/TNSs composites.

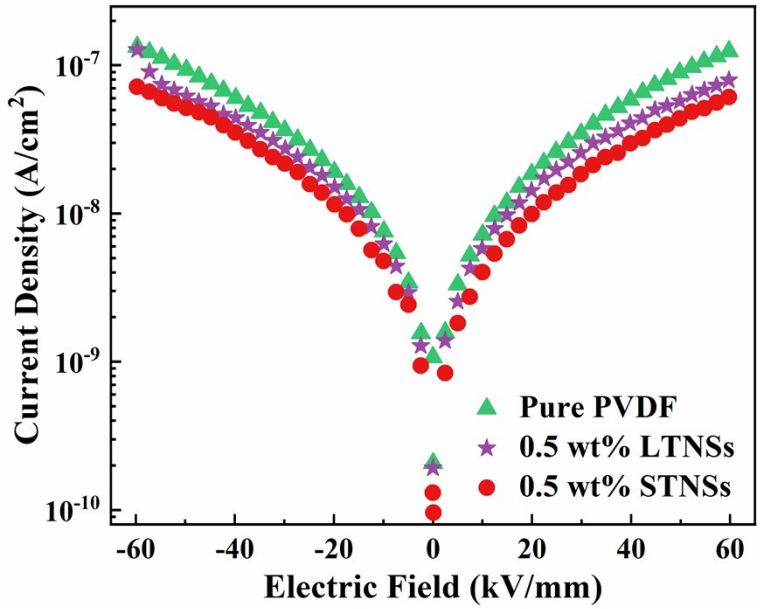

Figure S23. The current density at 60 kV/mm of PVDF/TNSs composites.

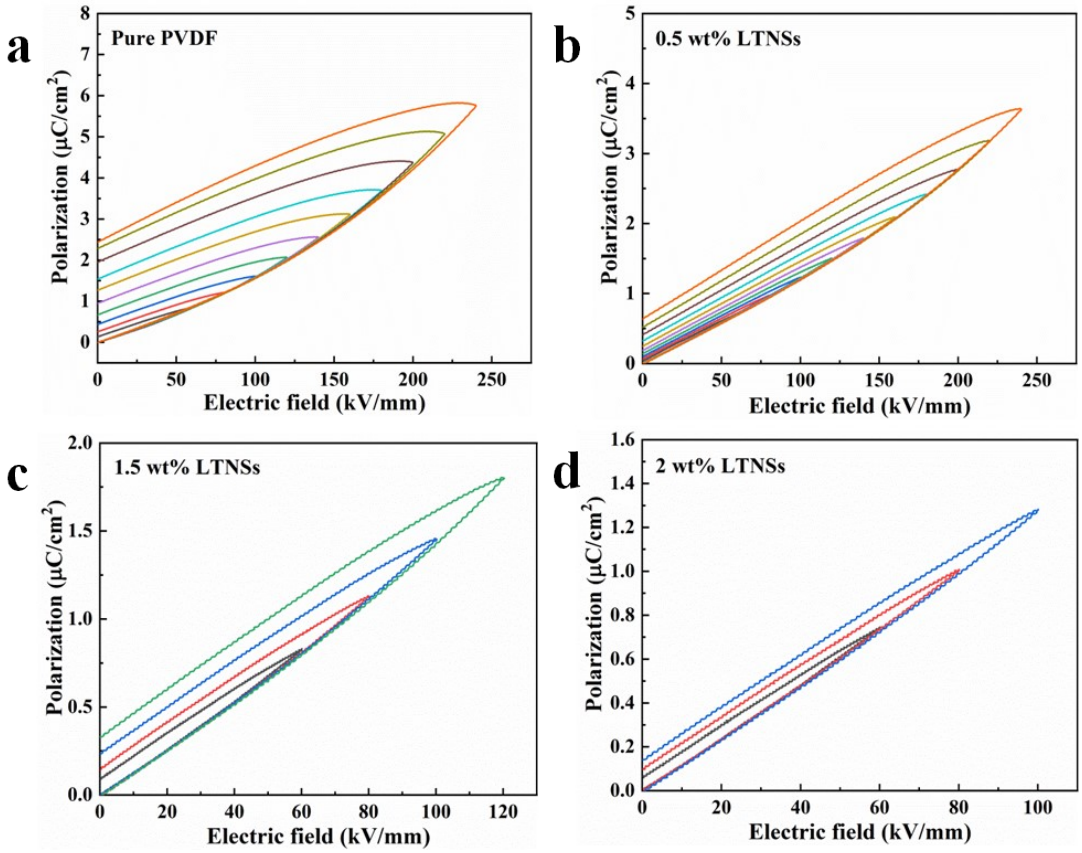

Figure S24. Hysteresis loops of PVDF/LTNSs composites with (a) 0 wt%, (b) 0.5 wt%, (c) 1.5 wt% and (d) 2 wt% fillers.

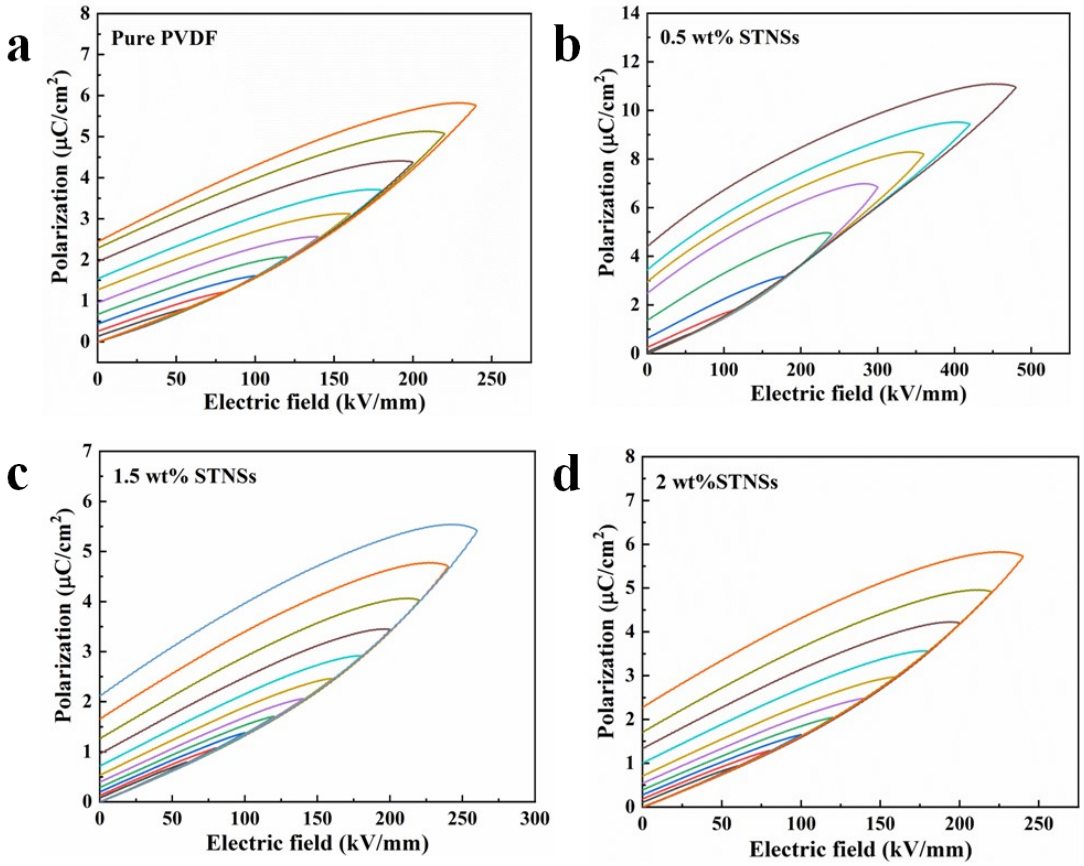

Figure S25. Hysteresis loops of PVDF/STNSs composites with (a) 0 wt%, (b) 0.5 wt%, (c) 1.5 wt% and (d) 2 wt% fillers.

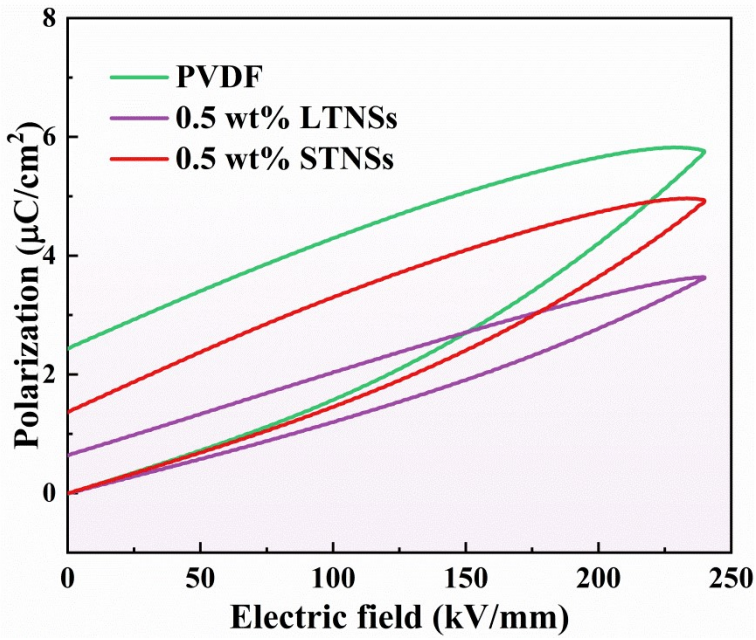

Figure S26. The polarization-electric field (*P*-*E*) loops of pure PVDF and PVDF/TNSs composites at 240 kV/mm.

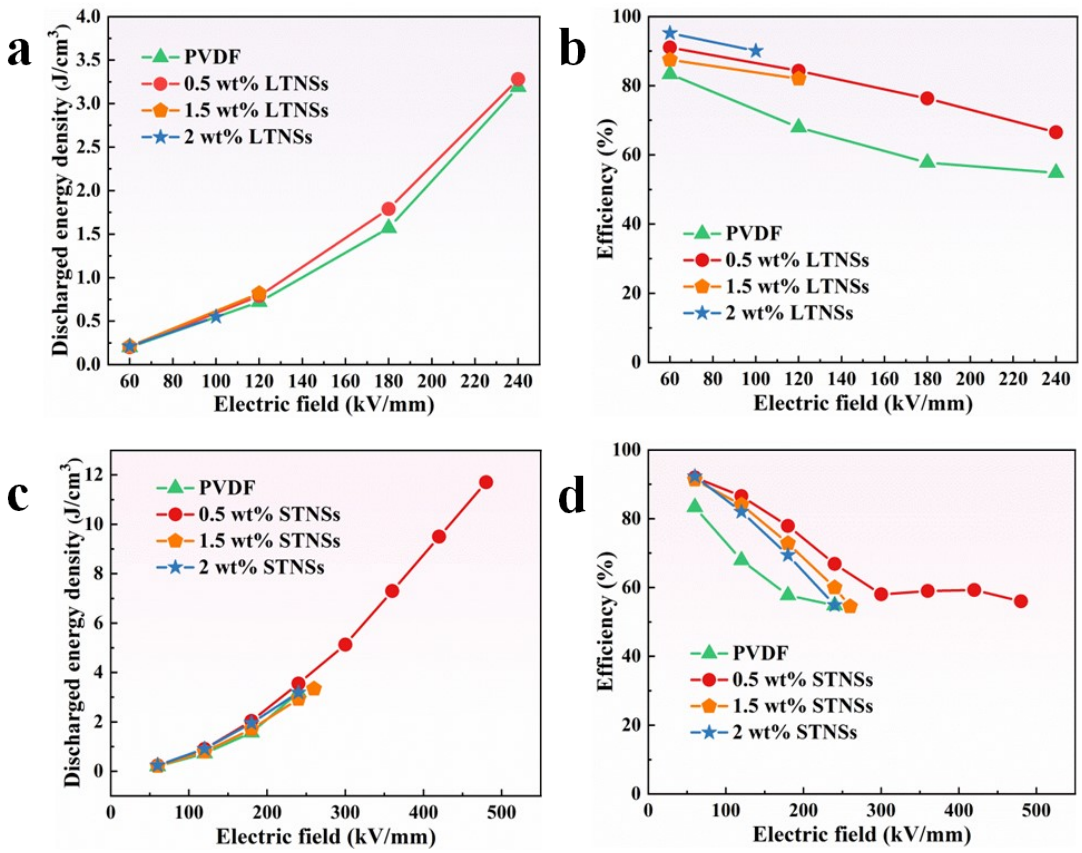

Figure S27. The discharged energy density (U_e) and efficiency (η) of PVDF/TNSs composites.

Table S1 DSC results, $F(\beta)$ and E_t of the composites.

Contents	T_m (℃)	T_c (℃)	ΔH_m (J/g)	X_c (%)	$F(\beta)$	E_t (nm)
0 wt%	161.9	137.1	43.7	41.8	52.3	2.13
0.5 wt% LTNSs	162.1	137.1	35.1	33.6	61.3	2.35
1.5 wt% LTNSs	165.8	138.8	35.1	33.6	60.4	2.55
2 wt% LTNSs	165.7	138.6	35.8	34.3	61.8	2.60
0.5 wt% STNSs	166.9	143.5	37.2	35.6	62.7	2.60
1.5 wt% STNSs	167.1	144.3	35.0	33.5	61.9	2.73
2 wt% STNSs	167.4	145.6	34.1	32.6	63.1	2.78

Reference

1. J. Hou, Y. Zheng, Y. Su, W. Zhang, T. Hoshide, F. Xia, J. Jie, Q. Li, Z. Zhao, R. Ma, T. Sasaki and F. Geng, J Am Chem Soc, 2015, 137, 13200-13208.
2. C. Zhu, J. Yin, J. Li, Y. Li, H. Zhao, D. Yue, L. Pan, J. Wang, Y. Feng and X. Liu, Journal of Applied Polymer Science, 2021, 138, 50244.
3. J. Li, J. Yin, C. Yang, N. Li, Y. Feng, Y. Liu, H. Zhao, Y. Li, C. Zhu and D. Yue, Journal of Polymer Science Part B: Polymer Physics, 2019, 57, 574-583.